AIAA JOURNAL
Vol. 33, No. 8, August 1995

Modeling High-Pressure Chemical Oxygen-Iodine Lasers

David L. Carroll*
University of Illinois at Urbana–Champaign, Urbana, Illinois 61801

The Blaze II chemical laser model was baselined to existing oxygen-iodine research assessment and device improvement chemical laser (RADICL) data. Mixing calculations for the RADICL nozzle indicate that higher iodine flow rates are necessary to maintain a significant fraction of the nominal performance as the helium flow rate is increased to raise the total pressure of the flow; this agrees with RADICL experimental data. Overall, the model is in very good qualitative and quantitative agreement with RADICL data as a function of increased He flow rate over a total pressure range of 70–130 Torr. This was accomplished only after the nominal $I_2^* + He \rightarrow I_2 + He$ rate constant was increased by an order of magnitude. To determine the set of five unknown parameters which best matched Blaze II model predictions with experimental data, a genetic algorithm technique was implemented to efficiently search the parameter space. This is the first known application of the genetic algorithm technique for modeling lasers, chemically reacting flows, and chemical lasers. Different reduced reaction/species sets were investigated; a 13-reaction, 10-species set gave excellent agreement and an 8-reaction, 8-species set gave very good agreement with the full reaction set.

Nomenclature

U = utilization, $\dot{x}_{O_2}/\dot{x}_{(Cl_2)_0}$
x_i = mole fraction of species i
$\dot{x}_i$ = molar flow rate of species i, moles/s
Y = yield, $O_2(^1\Delta)$/[total O_2]
β = titration ratio, $\dot{x}_{I_2}/\dot{x}_{O_2}$
ψ = diluent ratio, $\dot{x}_{(He)_{pri}}/\dot{x}_{(Cl_2)_0}$

I. Introduction

A NUMBER of papers have investigated issues associated with the operation of chemical oxygen-iodine laser (COIL) systems.[1] These include the required $O_2(^1\Delta)$ generators,[2–8] the ratio of I_2 to O_2 flow rates (titration) for optimal performance,[1] the energy transfer dynamics,[9] and the power extraction efficiency,[1] among others. Crowell and Plummer[10] addressed the issue of how the extracted power is affected by significant increases in the total pressure of the flow (up to approximately 120 Torr), but their power results were not in particularly good agreement with data because they used a premixed model for the laser cavity calculations. No one has addressed the issues of the extent of mixing, I_2 dissociation, small signal gain, power, and system performance when the total pressure of the flow is increased to levels greater than 120 Torr. If the total pressure of a COIL device can be increased significantly while maintaining the device's nominal performance, then it should be possible to reduce the size of pressure recovery systems. Typically, COIL devices have been operated in the total pressure range of 30–75 Torr; thus, high-pressure COIL devices are considered to be those having a total pressure in excess of 75 Torr. The effects of increased total pressure on mixing, kinetics, gain, and power must be analyzed with a reliable computer model. To accomplish this objective, the Blaze II laser simulation code[11] was modified to model a slit nozzle laser device with sidewall injection. The model was baselined to recent COIL power data[12] as a function of total pressure over the range 70–130 Torr. The baselined model was used to develop reduced reaction sets for use with more detailed three-dimensional computational fluid dynamic models. Finally, the baselined model was used to predict qualitative laser performance trends at higher pressure COIL operating conditions, approximately 205 Torr total pressure; no experimental data are available at this high a pressure.

Presented as Paper 94-2431 at the AIAA 25th Plasmadynamics and Lasers Conference, Colorado Springs, CO, June 20–23, 1994; received July 1, 1994; revision received Nov. 3, 1994; accepted for publication Nov. 10, 1994.

*Postdoctoral Research Associate, Department of Aeronautical and Astronautical Engineering. Member AIAA.

II. Blaze II Model for a Slit Nozzle Oxygen-Iodine Laser

The Blaze II code[11] was originally written to be as generic a chemical laser model as possible. Blaze II can treat arbitrary combinations of chemical species characterized by as many as 500 reactions and 40 species. Blaze II, which contains one-dimensional fluid dynamic equations whose mixing terms were derived from the two-dimensional equations that describe the mixing flowfield in a chemical laser cavity, can be used for axisymmetric and two-dimensional flows. Lasing may occur on a single atomic transition or on as many as 10 vibrational bands of a diatomic species. Rotational equilibrium is assumed. The run time is sufficiently short that extensive parametric studies can be performed in reasonably short times; a typical hydrogen-fluouride (HF) chemical laser run takes approximately 70 CPU s on an IBM RS/6000 computer, and a typical COIL run takes approximately 30 CPU s on the same machine. Although Blaze II was designed to be a robust code, it had not been used extensively to predict the performance of a COIL (single atomic transition) device. To validate the Blaze II model for COIL calculations, a number of premixed Blaze II calculations at a total pressure of 73 Torr were compared with calculations from Logicon Research and Development Associates (RDA) premixed RECOIL model.[13] Blaze II is capable of performing premixed and mixing calculations, but the RECOIL model only treats premixed flow. These Blaze II calculations were in very good agreement with the RECOIL calculations having the same initial conditions for the same device.[14]

Unless otherwise specified, all of the calculations made in this paper used the 33-reaction, 12-species set[13] listed in Table 1. All of the reactions tabulated are one-way reactions. The gain g of a COIL laser is given by[1,10,13]

$$g = \frac{7}{12}\left(\frac{A\lambda^2}{8\pi}\right)\phi(\nu)\left(N_{I^*} - \frac{1}{2}N_I\right) \tag{1}$$

where $\lambda = 1.315274 \times 10^{-4}$ cm, $A = 5.0\ s^{-1}$, N_{I^*} and N_I are the number densities of excited atomic iodine I^*, and ground state atomic iodine I, and the Voight line shape function $\phi(\nu)$ is given by

$$\phi(\nu) = (2/\Delta\nu_D)\,(\ell n 2/\pi)^{\frac{1}{2}}[1 - \mathrm{erf}(y)]\exp(y^2) \tag{2}$$

where

$$\Delta\nu_D = (2/\lambda)\sqrt{2RT\ell n 2/W} = 1.4492 \times 10^7\sqrt{T} \tag{3}$$

$$y = (\Delta\nu_L/\Delta\nu_D)\sqrt{\ell n 2} \tag{4}$$

$$\Delta\nu_L = \frac{T_{ref}}{T}P\sum_i \alpha_i x_i \tag{5}$$

Table 1 Full oxygen–iodine reaction set; 33 reactions, 12 species: I, I*, I_2, I_2*, He, H_2O, $O_2(^1\Delta)$, $O_2(^3\Sigma)$, $O_2(^1\Sigma)$, Cl_2, Cl, ICl

k								Rates, cm^3/molecule–s
1	$O_2(^1\Delta)$	+	$O_2(^1\Delta)$	→	$O_2(^1\Sigma)$	+	$O_2(^3\Sigma)$	2.50e-17
2	$O_2(^1\Delta)$	+	$O_2(^1\Delta)$	→	$O_2(^3\Sigma)$	+	$O_2(^3\Sigma)$	1.80e-17
3	$O_2(^1\Sigma)$	+	$O_2(^3\Sigma)$	→	$O_2(^1\Delta)$	+	$O_2(^3\Sigma)$	3.90e-17
4	$O_2(^1\Sigma)$	+	H_2O	→	$O_2(^1\Delta)$	+	H_2O	6.00e-12
5	$O_2(^1\Sigma)$	+	Cl_2	→	$O_2(^1\Delta)$	+	Cl_2	2.00e-15
6	$O_2(^1\Sigma)$	+	He	→	$O_2(^1\Delta)$	+	He	1.00e-17
7	$O_2(^1\Delta)$	+	$O_2(^3\Sigma)$	→	$O_2(^3\Sigma)$	+	$O_2(^3\Sigma)$	1.60e-18
8	$O_2(^1\Delta)$	+	H_2O	→	$O_2(^3\Sigma)$	+	H_2O	4.00e-18
9	$O_2(^1\Delta)$	+	Cl_2	→	$O_2(^3\Sigma)$	+	Cl_2	6.00e-18
10	$O_2(^1\Delta)$	+	He	→	$O_2(^3\Sigma)$	+	He	8.00e-21
11	I_2	+	$O_2(^1\Sigma)$	→	2I	+	$O_2(^3\Sigma)$	4.00e-12
12	I_2	+	$O_2(^1\Sigma)$	→	I_2	+	$O_2(^3\Sigma)$	1.60e-11
13	I_2	+	$O_2(^1\Delta)$	→	I_2*	+	$O_2(^3\Sigma)$	7.00e-15
14	I_2	+	I*	→	I	+	I_2*	3.50e-11
15	I_2^*	+	$O_2(^1\Delta)$	→	2I	+	$O_2(^3\Sigma)$	3.00e-10
16	I_2^*	+	$O_2(^3\Sigma)$	→	I_2	+	$O_2(^3\Sigma)$	5.00e-11
17	I_2^*	+	H_2O	→	I_2	+	H_2O	3.00e-10
18	I_2^*	+	He	→	I_2	+	He	4.00e-12
19	I	+	$O_2(^1\Delta)$	→	I*	+	$O_2(^3\Sigma)$	7.80e-11
20	I*	+	$O_2(^3\Sigma)$	→	I	+	$O_2(^1\Delta)$	1.0277e-10* exp(−401.4/T)
21	I	+	$O_2(^1\Delta)$	→	I	+	$O_2(^3\Sigma)$	1.00e-15
22	I*	+	$O_2(^3\Sigma)$	→	I	+	$O_2(^3\Sigma)$	3.50e-16
23	I*	+	$O_2(^1\Delta)$	→	I	+	$O_2(^1\Sigma)$	1.00e-13
24	I*	+	$O_2(^1\Delta)$	→	I	+	$O_2(^1\Delta)$	1.10e-13
25	I	+	I*	→	I	+	I	1.60e-14
26	I*	+	H_2O	→	I	+	H_2O	2.10e-12
27	I*	+	He	→	I	+	He	5.00e-18
28	I*	+	Cl_2	→	Cl	+	ICl	5.50e-15
29	I*	+	Cl_2	→	I	+	Cl_2	8.00e-15
30	I*	+	ICl	→	I_2	+	Cl	1.50e-11
31	I_2	+	Cl	→	I	+	ICl	2.00e-10
32	Cl	+	ICl	→	I	+	Cl_2	8.00e-12
33	I_2	+	2I	→	I_2	+	I_2	3.60e-30

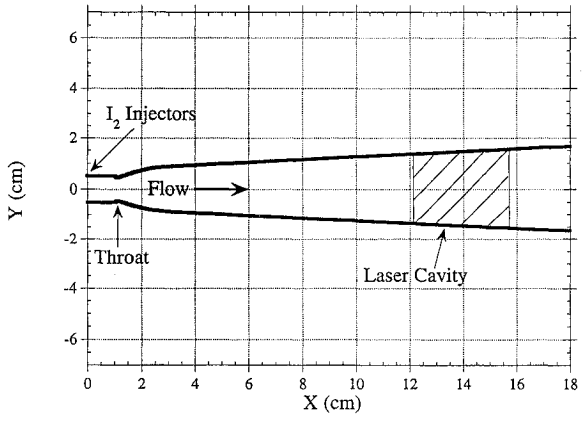

Fig. 1 RADICL nozzle and laser cavity used for high-pressure experiments and modeling.

R is the universal gas constant (8.3143×10^7 ergs/mole-K), W is the molecular weight of iodine (126.90447 gm/mole), T is the temperature in degrees Kelvin, T_{ref} is a reference temperature taken to be 295 K, P is the pressure in Torr, x_i is the mole fraction of species i, and the pressure broadening coefficients α_i in MHz/Torr (referenced to 295 K) are 4.4, 10.5, 7.3, 6.2, 20.6, 3.6, 3.6, and 4.7 for I, I_2, O_2, Cl_2, H_2O, He, N_2, and Ar, respectively.[10]

Blaze II was originally written to perform laminar or scheduled mixing of the primary and secondary streams, from a nozzle array, which mix in the laser cavity. In a single slit nozzle such as RADICL, Fig. 1, the mixing occurs in the nozzle as well as in the cavity.

The general flow geometry of the single-slit nozzle problem is illustrated in Fig. 2. Blaze II requires parallel flow by the primary (O_2), secondary (I_2), and mixed streams; therefore, the secondary flow of I_2, which is injected perpendicular to the primary flow in the research assessment and device improvement chemical laser (RADICL) nozzle, must be assumed to penetrate some distance into the nozzle and then be completely turned, Fig. 2. Thus, it is assumed that the injectors penetrate and block the primary flow such that the primary flow has a half-width of H_1 and the secondary flow has a half-width of H_2; note that $H_1 + H_2 = Y$, the half-height of the nozzle at any position X. The question of the initial value of $(H_2)_0$ for given flow conditions will be addressed later.

III. Mixing Predictions for Research Assessment and Device Improvement Chemical Laser Nozzle

Since the high pressure COIL experiments were performed with the RADICL nozzle, the modeling investigation focused on that nozzle. The geometry of the RADICL nozzle and laser cavity section are shown in Fig. 1. A schematic of the experimental setup is shown in Fig. 3. A detailed discussion of the experimental configuration is given in Ref. 10. Before any mixing calculations can be performed, the initial conditions for each stream must be specified. Blaze II requires the following inputs for each stream: the total mass flow rate, the mass fraction of each species, the pressure, the temperature, the Mach number, the initial height of the stream, and a reference diffusion coefficient. Since Blaze II is a quasi-two-dimensional mixing model, each stream has uniform conditions at each x position, i.e., it is not possible to input nonuniform species concentrations in each stream. To accurately simulate experimental conditions, RADICL experimental data were tabulated, plotted, and linear least square fits were used to determine certain input parameters as a function of the primary and secondary flow rates. This procedure was used to determine the utilization, the total temperature, and total pressure of the primary stream, and the total temperature and total pressure in the iodine heater cell.

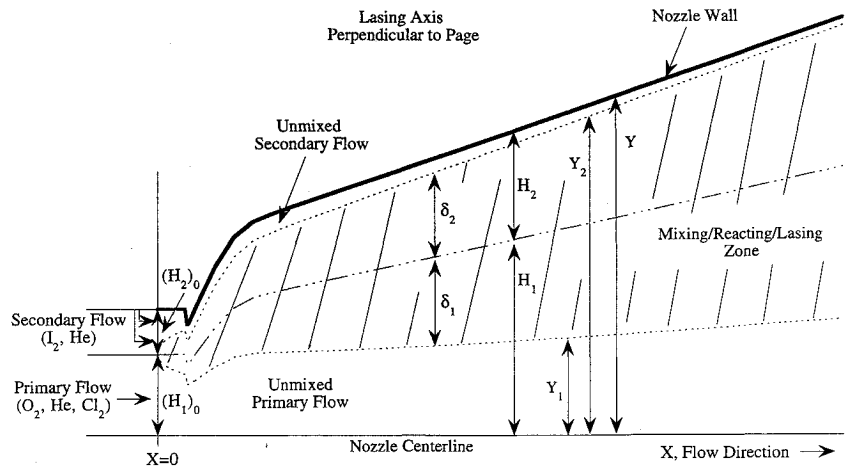

Fig. 2 Schematic of the Blaze II slit nozzle mixing model for half of a nozzle.

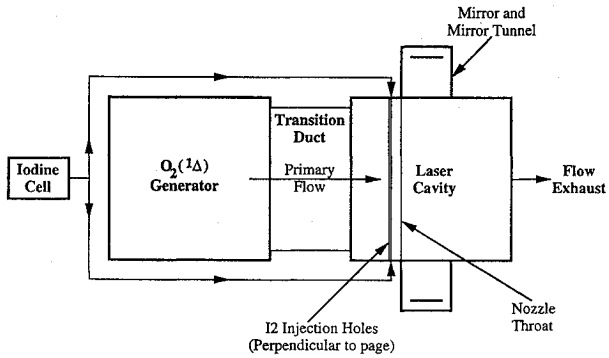

Fig. 3 Schematic of the RADICL experimental layout.

Since the secondary flow from the iodine heater cell passes through approximately 6 ft of tubing wrapped with heater tape (set at approximately 400 K) before actually entering the secondary reservoir manifold for the injectors, there will be a drop in temperature. The total temperature in the secondary manifold is approximated as the average of 400 K and the total temperature in the iodine cell, i.e., $(T_{\text{tot}})_{\text{sec}} = 0.5[(T_{\text{tot}})_{\text{cell}} + 400]$. Since there are several bends in the tubing through which the secondary flow passes from the iodine cell to the secondary manifold, there will also be a pressure drop. The pressure drop is approximated as being proportional to the temperature drop, i.e., $(P_{\text{tot}})_{\text{sec}} = (P_{\text{tot}})_{\text{cell}}[(T_{\text{tot}})_{\text{sec}}/(T_{\text{tot}})_{\text{cell}}]$. Based on these values of the secondary total pressure and temperature, an ideal isentropic mass flow can be computed for injectors having a geometric area of 1.7901 cm^2. The ideal calculated mass flow is significantly larger than the actual experimental flow rate; this phenomenon is typical for sonic injectors. As a consequence of the difference between actual and ideal flow rates, a discharge coefficient, $C_d (= \dot{m}_{\text{actual}}/\dot{m}_{\text{ideal}})$ is calculated and the injector diameters are adjusted accordingly, i.e., $D_{\text{eff}} = D_{\text{geom}}(C_d)^{\frac{1}{2}}$. This effective diameter of the injectors was used as the injector diameter for all subsequent calculations. For different flow conditions the discharge coefficient ranged between 0.6 and 0.7, but for most flow conditions it was approximately 0.65; discharge coefficients in this range are quite reasonable for sonic orifices.[15,16]

The penetration of the I_2 jets into the primary flow of O_2 must be estimated in order to calculate H_1 and H_2. The parameter of significance in the Cohen et al.[17] study of jet penetration into a crossflowing stream is the relative momentum flux of the two flows, $(\rho v^2)_i/(\rho v^2)_\infty$, where $(\rho v^2)_i$ is the momentum flux of the injectant stream, and $(\rho v^2)_\infty$ is the momentum flux of the primary crossflow stream. The Mach number of the primary flow upstream of the I_2 injectors is approximately 0.645, and the Mach number of the secondary flow at the exit of the sonic injectors is unity. Knowing the Mach number, the gas composition, and the total conditions, the static conditions of the two streams can be determined at the injectors. From the static conditions, the momentum flux ratio can be computed and the penetration can be found from the Cohen et al.[17] empirical fit to data;

$$\frac{H_{\text{top}}}{D}(1 + \cos\alpha) = 1.51\left[\frac{(\rho v^2)_i}{(\rho v^2)_\infty}\right]^{0.5} \tag{6}$$

where H_{top} is the top of the jet penetration height, D is the effective hole diameter (adjusted for any discharge coefficient), and α is the angle of injection relative to the channel wall. Since $\alpha = 90$ deg for the RADICL device, $(H_{\text{top}}/D)(1 + \cos\alpha) = (H_{\text{top}}/D)$ for the I_2 injectors. There are two rows of I_2 injectors in the plenum region of the RADICL nozzle. There are 115 large and 230 small injector holes on each side (top and bottom) of the nozzle plenum. The large and small I_2 injectors have geometric diameters of 0.032 and 0.016 in., respectively. The large holes have a spacing of 0.085 in. between their centerlines, and the small holes have a spacing of 0.0425 in. between their centerlines. The centerline of the row of large holes is 0.12 in. upstream of the centerline of the row of small holes. The centerline of the row of large injectors is considered to be $x = 0$ in the Blaze II modeling calculations. Equation (6) requires an effective hole diameter, therefore, the geometric diameters were adjusted for a discharge coefficient using the relation $D_{\text{eff}} = D_{\text{geom}}(C_d)^{\frac{1}{2}}$.

The next question is, how do these penetration heights relate to the value of $(H_2)_0$ required by Blaze II? Setting $(H_2)_0$ equal to the penetration height H_{top} is not realistic because there is primary flow passing between the individual three-dimensional jets, i.e., each jet may block flow to a height H_{top}, but there is no flow blockage between the jets. In essence, the ratio of $(H_2)_0$ to the half-height of the flow channel at $x = 0$, Y_0, represents the percentage of channel area blocked to the primary stream. For illustrative purposes, Fig. 4 shows the jets and their blockage of the primary flow. For generality it will be assumed that the jets expand by an average factor J_{exp} when they enter the lower pressure primary flow. The jets definitely expand, but the amount of expansion is uncertain. Reference 18 indicates that an underexpanded jet with a pressure ratio $[(P_0)_{\text{sec}}/P_{\text{pri}}]$ of approximately 6 (the ratio for the RADICL experimental conditions) has an expansion of approximately unity, i.e., very little expansion. If we consider simple quasi-one-dimensional fluid dynamic expansion for a $\gamma = 1.67$ fluid ($\gamma \approx 1.65$ for the He/I_2 secondary jets) from Mach 1 to a pressure ratio of $P_{\text{pri}}/(P_0)_{\text{sec}} \approx 1/6$, the area ratio A/A^* is $\approx$1.32. Since the jet expands three dimensionally, the effective diameter of the expanded jet goes as the square root of the area ratio, $D_{\text{exp}}/D \approx 1.15$. Since the jet would expand to this value over the full penetration height, the average expansion is about $1.075 \approx 1.1$. Thus, $J_{\text{exp}} = 1.1$ will be used for these Blaze II calculations. If the area between injector centerlines from the nozzle wall to the nozzle centerline is considered, the area of primary flow just before the injectors is

$$A_{\text{available}} = SY \tag{7}$$

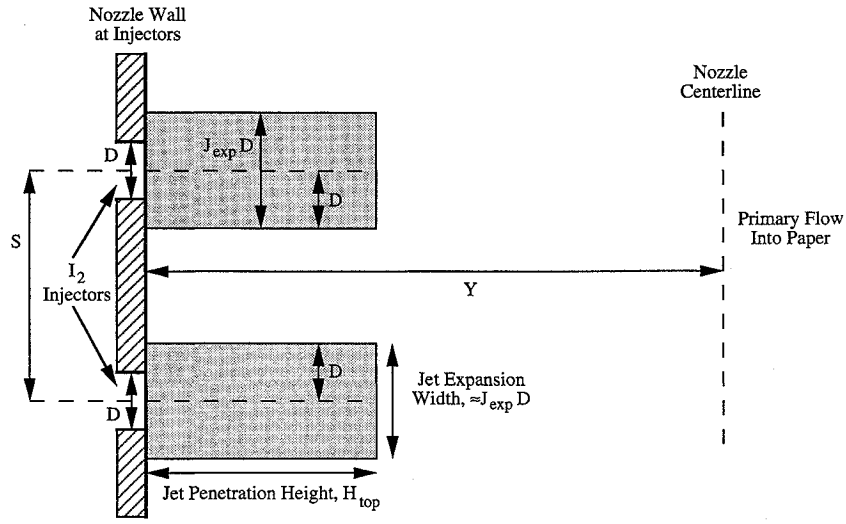

Fig. 4 Schematic of the blockage of the primary crossflow by iodine injectors oriented perpendicular to the primary flow.

where S is the spacing between injector centerlines. The area blocked by the injectors is

$$A_{\text{blockage}} = J_{\text{exp}} D H_{\text{top}} \tag{8}$$

Therefore, the fraction of the available primary flow area which is blocked is

$$B = \frac{A_{\text{blockage}}}{A_{\text{available}}} = \frac{J_{\text{exp}} D H_{\text{top}}}{SY} \tag{9}$$

The spacing between injectors S for the small and large holes is 0.0425 and 0.085 in., respectively. Equation (9) can then be used to calculate the flow blockage by the small and large injectors as a function of jet penetration height. Since the flow blockage by the large holes is greater than that by the small holes, it is reasonable to assume that the flow which passes around the large injector jets will manage to pass around the small injector jets. Thus, it is reasonable to assume that under these flow conditions the large jets represent the major contributor to the primary flow blockage. Since we are trying to model a three-dimensional flow with a quasi-two-dimensional model, we need to determine the initial relative heights of the parallel primary $(H_1)_0$ and secondary $(H_2)_0$ streams, Fig. 2. The two-dimensional equivalent height of the jet penetration (the secondary flow) is the product of the channel half-height at $x = 0$, Y_0, and the fraction of the primary flow blocked by the jets B,

$$(H_2)_0 = Y_0 B \tag{10a}$$

The remainder of the channel half-height represents the primary flow

$$(H_1)_0 = Y_0(1 - B) = Y_0 - (H_2)_0 \tag{10b}$$

For the RADICL nozzle, $Y_0 = 0.2005$ in. and the values for $(H_1)_0$ and $(H_2)_0$ are determined from the momentum flux ratio (which gives the jet penetration height) and Eqs. (9) and (10).

Now that reasonable values for $(H_1)_0$ and $(H_2)_0$ are determined we need to find reasonable values for the flow properties (pressure, temperature, and Mach number) of the primary and secondary streams at $x = 0$, Fig. 2. There is no experimental data for the injector region and since the actual flow involves complicated three-dimensional effects (including flow between injector jets), it is not possible to directly determine the average flow properties of each stream for input to Blaze II. As such, the pressure and temperature of the primary and secondary streams were assumed to be equal to the values appropriate for a premixed (plug flow) calculation. In a one-dimensional nozzle at a position inj (e.g., the I_2 injectors),

$$\frac{A_{\text{inj}}}{A_*} = \frac{1}{M_{\text{inj}}}\left[\left(\frac{2}{\gamma+1}\right)\left(1 + \frac{\gamma-1}{2} M_{\text{inj}}^2\right)\right]^{(\gamma+1)/2(\gamma-1)} \tag{11}$$

For the RADICL device, as the flow rates are varied, γ is approximately constant (γ increases from approximately 1.58 to 1.63 as He is added). From Eq. (11), since $A_{\text{inj}}/A* = \text{const}$ for a given nozzle and $\gamma \approx$ const as He is added to the flow, then $M_{\text{inj}} \approx$ const; for the RADICL nozzle, $M_{\text{inj}} \approx 0.645$. The temperature of the premixed flow is assumed to be approximately the molar temperature average of the two streams at $M = 0.645$,

$$T_{\text{inj}} = \{[(\dot{x}T_{M=0.645})_{\text{pri}} + (\dot{x}T_{M=0.645})_{\text{sec}}]/(\dot{x})_{\text{tot}}\} \tag{12}$$

where $\dot{x}$ is the molar flow rate of all gases in stream i, the subscript pri is for the primary O_2 stream, the subscript sec is for the secondary I_2 injectant stream, and the subscript tot represents the entire flow as a premixed stream. The initial pressure for the calculation at the injectors is given by

$$P_{\text{inj}} = \frac{\dot{m}_{\text{tot}}}{M_{\text{inj}} A_{\text{inj}}} \sqrt{\frac{R T_{\text{inj}}}{\gamma_{\text{tot}} W_{\text{tot}}}} \tag{13}$$

where A_{inj} is the total flow area at the injectors [$= 2Y_0 L_g = 2$ (0.2005 in.)(10.0 in.) $= 4.010$ in.^{2}, where L_g is length of the gain region, i.e., the nozzle length]. Then, using the continuity and state equations, the initial Mach number of each stream i (primary and secondary) can be determined from

$$M_i = \frac{\dot{m}_i}{P_{\text{inj}} A_i} \sqrt{\frac{R T_{\text{inj}}}{\gamma_i W_i}} \tag{14}$$

where A_i is the flow area of stream i [$=2(H_i)_0 L_g = (H_i)_0$ (10.0 in.)]. When the primary flow is blocked by the injector jets, its flow area decreases and the Mach number of the primary increases. The secondary is subsonic outside of the "shock bottle"[18] formed by the underexpanded injector jet. For all of the RADICL calculations, it turns out that the Mach number of the primary stream was larger than that of the secondary.

The reference diffusion coefficients for the primary and secondary streams must still be determined. Using a gas properties code written and provided by Driscoll,[19] the species composition, pressure, and temperature of the two streams were used as input to determine the nominal laminar diffusion coefficients at $x = 0$; the diffusion coefficient calculation is based on Ref. 20. One question which arises is whether or not it is appropriate to use laminar diffusion coefficients for cases with a total pressure as high as 200 Torr. Calculations of the Reynolds number for the worst conditions modeled (a flow with a total pressure of 205 Torr at the end of the laser cavity) indicated that $Re_x \approx 1.4 \times 10^5$ which corresponds to an $Re_\delta = 5(Re_x)^{\frac{1}{2}} \approx 1900$ (Ref. 21). These values are well below the critical values of $Re_{x,\text{crit}} \approx 3.2 \times 10^5$ and $Re_{\delta,\text{crit}} \approx 2800$ of Ref. 21 for a flat plate. $Re_\delta \approx 1900$ is also less than the value of $Re_{\delta,\text{crit}} \approx 2300$ for a pipe.[21] Therefore, even for a flow with a total pressure of approximately 200 Torr, the flow should still be laminar and the use of laminar diffusion coefficients is appropriate. However, turbulence may become an issue at flow total pressures of around 300 Torr.

Because the I_2 injectors enhance mixing, the nominal laminar diffusion coefficients are not appropriate for RADICL. A surface stretching scheme proposed by Driscoll[22,23] was used to estimate a diffusion coefficient multiplier (DCM). In Ref. 23, very good agreement with experimental data was obtained using Blaze II and a DCM to model the complex mixing processes which occur in chemical lasers with injector jets. Driscoll[22,23] suggests that an appropriate DCM is

$$\text{DCM} \approx \psi_r^2 = 1 + (H/L_r)^2 \tag{15}$$

where ψ_r is a constant reference value of the surface extension ratio, H is the jet penetration height, and L_r is the gas trip (injector) jet spacing ($L_r = S$, defined earlier). For these modeling calculations, the jet penetration height is taken to be $H = H_{\text{top}}$. There are two sets of injectors, large and small. Because of the geometry of the problem (large injectors are twice the diameter of the small injectors, but there are twice as many small injectors), the DCM for each set of injectors is the same. The surface stretching mixing enhancement scheme is represented by an increase in the contact area between the two streams. Because the primary flow which passes between the large injector jets should also pass between and over the small injector jets, it is felt that the enhanced mixing effects of the set of large injectors should not be significantly improved by the second set of injectors, i.e., only the large set of injectors will be considered to enhance the mixing. Multiplying the nominal laminar diffusion coefficients calculated earlier by the DCM of the large injector jets gives the necessary reference diffusion coefficients for the primary and secondary streams. For the flow conditions studied in this paper, the DCM ranged between 1.8 and 3.2; the peak power points typically had a DCM of 2.8.

Blaze II requires the following inputs for each stream: the total mass flow rate, the mass fraction of each species, the pressure, the temperature, the Mach number, the initial height of the stream, and the reference diffusion coefficient. With the exception of the oxygen yield [which gives the relative mass fractions of $O_2(^1\Delta)$ and $O_2(^3\Sigma)$] and water vapor in the primary stream at the I_2 injectors, all of these initial conditions for Blaze II are accurately measured experimentally (mass flow rates) or can be approximately determined (from the previous discussion). There are experimental values for the oxygen yield, but unfortunately this yield diagnostic is not very accurate. Hence, there is a great deal of uncertainty in the oxygen yield in the plenum of the RADICL nozzle; experimental values range from 0.22 to 0.55 (Refs. 12, 24, and 25). The amount of water vapor is believed to be in the range of 0.01–0.10 moles/s (Refs. 12, 24, and 25). Therefore, a study of the effects of changing the yield and the amount of water vapor was undertaken. The objective of this investigation was to determine a combination of the yield and water vapor parameters which best predicted the experimental outcoupled power of the all of the experimental data. Since there is a broad range in the yield and H_2O parameters, to narrow the range of likely values of the parameters, three data points were selected for initial studies: the nominal $\psi = 3$ [ψ is the diluent ratio $= \dot{x}_{(\text{He})_{\text{pri}}}/\dot{x}_{(\text{Cl}_2)_0}$], $\beta = 0.016$ [β is the titration ratio $= \dot{x}_{\text{I}_2}/\dot{x}_{\text{O}_2} = \dot{x}_{\text{I}_2}/U(\text{Cl}_2)_0$ where U is the utilization of the Cl_2 flow rate into the oxygen generator] case, the $\psi = 6$, $\beta = 0.016$ case, and the $\psi = 6$, $\beta = 0.025$ case.

First, nominal input conditions were chosen for the nominal $\psi = 3$, $\beta = 0.016$ case and the yield was varied between 0.35 and 0.60 for three different values of the water vapor (0.01, 0.05, and 0.10), Fig. 5. For a large water vapor flow rate of 0.10 moles/s, it was not possible to match the experimental power of 4400 Watts with a yield in the range 0.22–0.55, Fig. 5. For a medium value of water vapor (0.05 moles/s), the experimental power was approximately matched with a yield of 0.55. For a low value of water vapor (0.01 moles/s), the experimental power was approximately matched with a yield of 0.42. The fact that the nominal power for the $\psi = 3$ case can be obtained by varying either the yield or the water vapor flow rate indicates that an accurate measurement of either should allow the other to be determined with modeling predictions. It is important that future experiments accurately measure at least one of these two current unknowns; of course, an accurate measurement of both the yield and the water vapor in the plenum would be best.

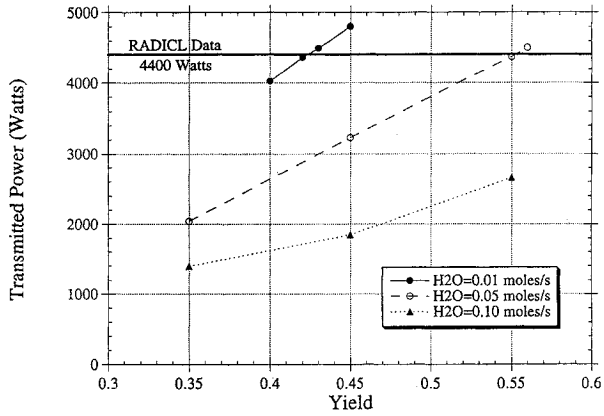

Fig. 5 Transmitted power vs yield for three different water vapor flow rates for the nominal $\psi = 3$, $\beta = 0.016$ case.

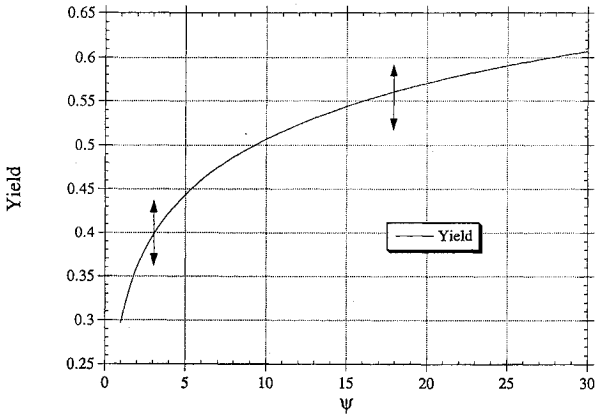

Fig. 6 Yield vs ψ (from Ref. 24) curve adjusted upwards or downwards so that the value of yield at $\psi = 3$ matches the yield which predicts the nominal power.

Given the range in yield of 0.22–0.55 from an inaccurate diagnostic, a reasonable guess for the yield is 0.40 for the $\psi = 3$ case.[12,24,25] The yield changes with ψ as shown in Fig. 6.[10,24] For Blaze II power calculations, the curve illustrated in Fig. 6 was shifted upwards or downwards so that the yield at the nominal $\psi = 3$ value was the same as that which matched the nominal power of 4400 W for a given water vapor flow rate. For example, the curve was shifted upwards by 0.02 (=0.42 − 0.40) for the 0.01 moles/s water vapor flow rate case and by 0.15 (=0.55 − 0.40) for the 0.05 moles/s water vapor flow rate case; the shape of the curve was not altered. A calculation was then run for the $\psi = 6$, $\beta = 0.016$ case with a yield of 0.55 and water vapor of 0.05 moles/s to see if Blaze II agreed with data. Blaze II predicted an increase in power to 5497 W whereas the data showed a very large decrease in power to approximately 200 W, Fig. 7. Similarly, a calculation was run for the $\psi = 6$, $\beta = 0.016$ case with a yield of 0.42 and water vapor of 0.01 moles/s to see if Blaze II agreed with data. Blaze II predicted an increase in power to 4804 W. At this point, not only was Blaze II not agreeing with the data, it was also predicting the wrong trend in the power regardless of significantly different values of yield and water vapor content.

By varying only the yield and water vapor, it was impossible to produce good agreement with data for different mass flow rates. Therefore, to obtain better agreement with the data as pressure was increased, the effects of various assumptions made in determining the input for Blaze II were investigated. First, one assumption is that the injector jets penetrate into the primary flow to a distance H_{top} based on Ref. 17 data, where H_{top} corresponds to the point where the species profile of the jets goes to zero. Another possibility is to define the jet penetration height as the centroid of the species profile, H_{mid}. When H_{mid} was used instead of H_{top} the predicted power for the $\psi = 6$ case was still greater than the $\psi = 3$ case rather than a significant decrease (not shown). Second, it was assumed that

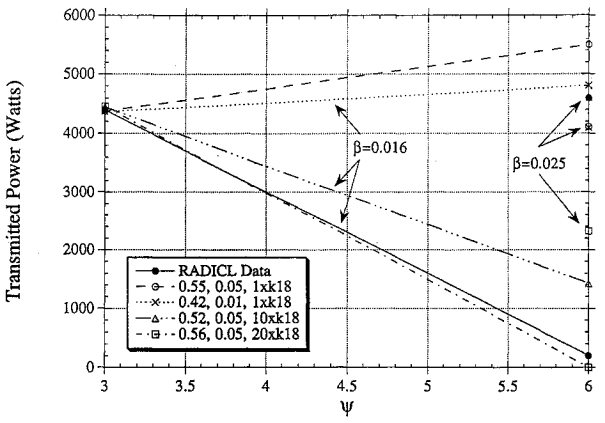

Fig. 7 Transmitted power vs ψ as a function of the yield at $\psi = 3$, the water vapor flow rate, and the rate constant k_{18}: lines denote $\beta = 0.016$, and the individual points at $\psi = 6$ are for $\beta = 0.025$.

the injector jets were expanding by an average factor of 1.1. When J_{exp} was set to as large as a factor of two, the predicted power still increased from the $\psi = 3$ case to the $\psi = 6$ case (not shown). Third, it was assumed that the secondary injector jets did not significantly affect the enhanced mixing caused by the primary injectors, i.e., the DCM was determined from only the primary injectors. To simulate the effects of further enhanced mixing by the secondary injectors, the DCM was increased by an arbitrary exponent

$$\mathrm{DCM} = (\mathrm{DCM})^{\mathrm{DCM_{exp}}} \tag{16}$$

where $\mathrm{DCM_{exp}}$ ranged between 1.0 and 2.0. The effects of enhancing the mixing beyond the a priori assumption ($\mathrm{DCM_{exp}} = 1.0$) did not reverse the predicted trend of increased power from the $\psi = 3$ case to the $\psi = 6$ case (not shown).

At this point, there are no other obvious assumptions that can be investigated which might produce agreement with data. It is possible to argue that the Blaze II quasi-two-dimensional mixing scheme is inadequate to model the performance of a laser with a three-dimensional flowfield. However, since the most obvious assumptions which were investigated all dealt with mixing, and since none of these assumptions when tested produced the experimental trend of decreasing power from the $\psi = 3$ case to the $\psi = 6$ case, it seems unlikely that the quasi-two-dimensional mixing model of Blaze II could be the only factor preventing the model from giving reasonable agreement with data. In fact, the Blaze II model has been extensively used in the past to model the performance of complicated HF mixing lasers as a function of different flow rates with quite reasonable agreement[23,26–28]; this suggests that there may be some other mechanism preventing agreement with the RADICL data. The problem appears to be related to increased total pressure by the addition of He. This raises the question of whether a chemical rate constant for a He reaction should be adjusted. The only rate constant involving He which is significantly large is that for $I_2^* + He \rightarrow I_2 + He$, rate k_{18} in Table 1. When the agreed upon COIL kinetics package in Ref. 29 was consulted, it was found that this reaction's rate constant has a low degree of confidence. Therefore, any adjustments to this rate constant within an order of magnitude should not be unreasonable. Recent data for this rate constant is discussed later.

The 0.05 moles/s flow rate, yield = 0.55, $J_{exp} = 1.1$, jet penetration to H_{top}, $\mathrm{DCM_{exp}} = 1.0$ conditions were used to investigate the effects of adjusting the rate constant k_{18}. When k_{18} was increased by a factor of 10, the yield was lowered to 0.52 to match the $\psi = 3$ power, the slope of the power vs ψ line was negative and approximately matched the slope of the data, Fig. 7. When k_{18} was increased by a factor of 20, the yield was increased to 0.56 to match the $\psi = 3$ power, and the predicted power was zero for the $\psi = 6$ case; the power vs ψ line was negative and approximately matched the slope of the data, Fig. 7. When β is increased to 0.025 for the $\psi = 6$ case, the data indicated an increase in power to 4600 W. For the $\beta = 0.025$, $\psi = 6$ conditions, the predicted power for the 0.52 yield/10 $\times$ k_{18} case was 4608 W, and the predicted power for the 0.56 yield/20 $\times$ k_{18} case was 2324 W, Fig. 7. It is clear that the 0.52 yield/0.05 H_2O/10 $\times$ k_{18} case shows promise for reasonable agreement with the entire data set. However, this was possible only by adjusting the rate constant k_{18}.

Now that the Blaze II model is in rough agreement with three data points, how well does it agree with other data for different flow rate combinations? In fact, the yield/H_2O/k_{18} multiplier parameter set of 0.56/0.05/10 does not produce particularly good overall agreement with data. The question then becomes, what combination of these three parameters would provide good overall agreement? Thus began an extensive search for a parameter set which minimized the differences between the predicted powers and the data as a function of the flow rates. If the parameters are descretized into increments, with reasonable yields running between 0.20 and 0.60 (in 0.01 increments), water vapor flow rates of 0.01 to 0.10 moles/s (in 0.01 increments), and a k_{18} multiplier somewhere between 1 and probably 20 (in increments of 1), the parameter space has around 10,000 possible permutations. If we also consider the possibility that J_{exp} could run between 1.0 and 2.0 and that there could be mixing enhancement from the secondary jets such that $\mathrm{DCM_{exp}}$ runs from 1.0 to 2.0, we are left with five parameters having some 1,000,000 possible permutations. To say the least, the task of searching this parameter space for a global or local minimum is daunting.

To tackle this problem, two significant additions were made to the Blaze II model. First, to facilitate the ease of making many calculations, a subroutine was added to the Blaze II model which creates the required COIL input deck automatically; previous calculations were a little tedious because a change in ψ and/or β was entered into a Microsoft Excel worksheet and all of the resulting flow rates were then manually typed into the normal Blaze II input deck (this also caused a number of calculations to be rerun due to the inevitable typing errors). The gas properties code used to compute the reference diffusion coefficients is now part of this new subroutine so that these coefficients and the DCM are automatically computed. The primary inputs to this subroutine are the five unknown parameters: the yield at $\psi = 3$, the primary flow rate of H_2O vapor, the multiplier for k_{18}, the jet expansion factor J_{exp}, and the DCM exponent $\mathrm{DCM_{exp}}$. Other inputs which can be altered depending on which experimental conditions are to be modeled are ψ, β, and the initial Cl_2 flow rate. All of the power calculations were made for a 92% reflective outcoupler, a 99.5% total reflector, and each mirror was assumed to have a 0.25% absorption/scattering loss. Distributed loss was not included in any of these calculations. The secondary flow rate of He was adjusted during the experiments to maintain approximately the same jet penetration. This increase in the secondary flow rate of He is approximated in the model as a simple function of the diluent ratio based on experimental data. Unless otherwise noted,

$$\text{sec He flow rate} = 0.65 + 0.10(\psi - 3)\ \text{moles/s} \tag{17}$$

This relation is approximately the same as a least squares fit to data. Second, and perhaps most importantly, once the Blaze II model was automated for many calculations based on the five parameters, a genetic algorithm[30,31] technique was coded and implemented to search the parameter space and minimize the differences between the predicted and experimental powers. One efficient algorithm that is robust enough to search for a global minimum given this highly nonlinear chemical laser model in this highly multimodal phase space (many local minimum) is the genetic algorithm.[31] To minimize required computer time while retaining a broad range of flow rates, five data points were chosen as a representative sample of the entire data set ($\psi = 3, \beta = 0.016$; $\psi = 6, \beta = 0.016$; $\psi = 6, \beta = 0.025$; $\psi = 10.33, \beta = 0.0317$; $\psi = 9.64, \beta = 0.0418$). Approximately 4 days of continuous running on an IBM RS/6000 computer was required to find a minimum for these five data points. Since it would take too much computer time to find a global minimum for the entire data set (43 data points), the best result found for the five data points is probably not the global minimum, but it is believed to be reasonably close. This is the first known application of the genetic algorithm technique for modeling lasers, chemically reacting flows, and chemical lasers.

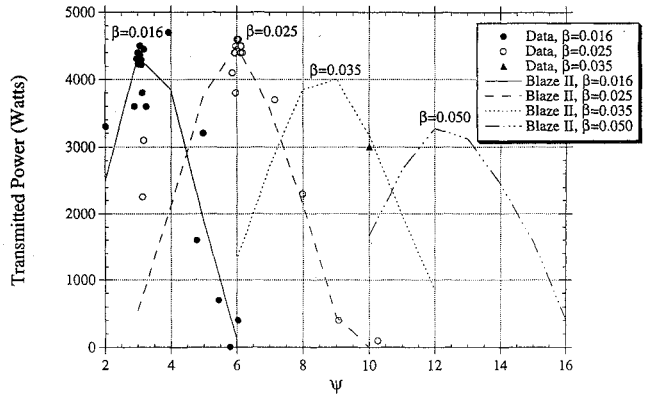

Fig. 8 Transmitted power as a function of ψ for different values of β; Blaze II parameters are a yield of 0.53 at ψ = 3, 0.08 H_2O, 12 × k_{18}, J_{exp} = 1.1, and DCM_{exp} = 1.0.

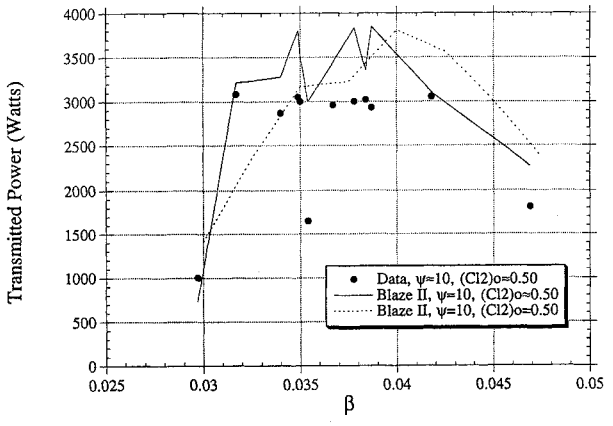

Fig. 9 Transmitted power as a function of β for $\psi \approx 10$; Blaze II parameters are a yield of 0.53 at ψ = 3, 0.08 H_2O, 12 × k_{18}, J_{exp} = 1.1, and DCM_{exp} = 1.0.

The parameters which gave the best overall agreement with the data were a yield at $\psi = 3$ of 0.53, a water vapor flow rate of 0.08 moles/s, a k_{18} multiplier of 12, $J_{exp} = 1.1$, and $DCM_{exp} = 1.0$. It is very interesting that despite the flexibility of the algorithm to find values of J_{exp} and D_{exp} between 1.0 and 2.0, that the algorithm found the initial a priori assumed values of 1.1 and 1.0, respectively, to give the best overall agreement. In fact, the combination of the first three parameters 0.53/0.08/12 is not very far removed from the previously determined rough estimate of 0.52/0.05/10. Nontheless, the genetic algorithm found a parameter set which was a better match than any which were determined by earlier personal search attempts.

The best overall agreement with data was obtained with a k_{18} multiplier of 12. Using an experimental technique outlined in Refs. 9 and 32, Heaven[33] recently measured the rate of vibrational relaxation of I_2 in the presence of He from $v'' = 23 \rightarrow v' = 22$ to be 1.8×10^{-10} cc/molecule-s. Using an I_2 relaxation simulation model provided by Heaven,[33] the $I_2^* + He$ deactivation rate k_{18} should be in the range of 1.1×10^{-11}–2.3×10^{-11} under typical laser cavity flow conditions (5 Torr and 150 K); this is a factor of approximately 3–6 above the original assumed rate of 4×10^{-12}. Although Heaven's data indicate a rate which is about a factor of 2 smaller than the factor of 12 increase deduced in this study, there is definitely agreement that the nominal $I_2^* + He$ deactivation rate is too slow. As a possible explanation of the discrepancy between the results of this study and Heaven's data, it has been suggested that the $I_2^* + O_2(^1\Delta) \rightarrow 2I + O_2(^3\Sigma)$ dissociation reaction k_{15} may be too fast.[33] If this dissociation reaction were slowed down by roughly a factor of 2 in conjunction with a factor of 6 increase in the $I_2^* + He$ deactivation rate, the effects may be similar to those of increasing the $I_2^* + He$ deactivation rate by a factor of 12. From Ref. 29 the nominal k_{15} dissociation reaction rate has a low to medium degree of confidence; as such, this reaction is currently being investigated.[33]

The agreement between data and Blaze II with the 0.53/0.08/12/1.1/1.0 parameter set is illustrated in Figs. 8 and 9. Figure 8 shows excellent agreement between data and Blaze II as a function of ψ for three different values of β. The model not only predicts the power very well, but also the upward and downward trends. Figure 9 shows the predicted power as a function of β for $\psi = 10$; at first glance it appears that the agreement with data is reasonable but not nearly as good as in Fig. 8. However, there are subtleties which must be noted. First, the dashed curve in Fig. 9 is for the case where ψ is exactly equal to 10 and the $(Cl_2)_0$ flow rate is exactly 0.50 moles/s. In fact, the data have a number of subtle variations (typically no greater than 5%, but occasionally as large as 25%) in the flow rates of primary He, $(Cl_2)_0$, I_2, and secondary He. When these small variations are used in computing the initial conditions for Blaze II, the solid curve shows significantly better agreement with data, Fig. 9 (consider the $\beta = 0.0317$ and 0.0418 points as well as those in between); this demonstrates the ability of Blaze II to track significant changes in performance due to seemingly minor variations in flow conditions. There are also significant variations in the pressure and temperature of the primary and secondary flows (not shown); it is quite possible that these variations, which were not included in the calculation of the initial conditions, may account for the three unexplained peaks which are approximately 20% higher than data, Fig. 9; i.e., if the pressure and temperature variations were included in the calculation of the initial conditions, then the peaks may drop into better agreement with the data. It is important to note that the deduced parameter set was optimized for only 5 of the 43 data points and that the same parameter set gave very good agreement with the other 38 data points which have significant flow rate variations. Regardless of any minor discrepancies, Figs. 8 and 9 suggest that Blaze II can now be used with some degree of confidence to make realistic qualitative predictions of COIL performance trends for the RADICL nozzle.

Mixing COIL calculations for the RADICL nozzle indicate that higher iodine flow rates are necessary to obtain a significant fraction of the nominal performance as ψ is increased to raise the total pressure of the flow, Fig. 8; this agrees with RADICL experimental data. The current experimental setup for RADICL limits the maximum I_2 flow rate to approximately 20 mmoles/s (Ref. 12), which corresponds to a value of β of approximately $\beta = 0.050$ for the nominal $(Cl_2)_0$ flow rate of 0.50 moles/s. The predicted performance as a function of ψ for $\beta = 0.050$ is shown in Fig. 8. The peak power of 3271 W occurs at a diluent ratio of $\psi = 12$. The trend appears to be a decrease in the maximum power obtainable as the diluent ratio (ψ) increases. Nontheless, the $\psi = 12$, $\beta = 0.050$ case corresponds to a generator total pressure of 142 Torr which is significantly greater than the nominal $\psi = 3$, $\beta = 0.016$ generator total pressure of 72 Torr and the predicted power level is still 74% of the nominal power. For the maximum experimentally obtainable value of $\beta = 0.050$ with the existing hardware, the predicted power dropped to zero (not shown) when ψ was raised to 20. Since we wish to operate at as high a total pressure as possible, the next question is how can the performance of the existing hardware be improved at higher generator total pressures?

Calculations (not shown) at a total pressure of 205 Torr ($\psi = 20$) were run to determine qualitative trends which should improve high-pressure performance. These calculations indicated that for the $\psi = 20$ case a significant reduction in the secondary He flow rate (worse penetration and mixing) led to higher power; why? This result is believed to be a consequence of the very high He concentrations at $\psi = 20$; the cumulative concentrations of mixing with the $\psi = 20$ core flow and the secondary He deactivates I_2^* too rapidly to permit sufficient gain build up. For the $\psi = 20$ case, when the secondary He flow rate is reduced and, consequently, the penetration and mixing rates are also reduced, the gain can build up sufficiently for lasing, albeit in a restricted region of the lasing cavity (because of reduced penetration and mixing). These calculations indicate that it should be possible to obtain lasing at a total pressure of at least 205 Torr; however the predicted power level is still lower than desired (approximately half of the nominal 4400 W), so the question of how to improve this performance remains.

Table 2 Reduced oxygen–iodine reaction set; 13 reactions, 10 species: I, I*, I_2, I_2*, He, H_2O, $O_2(^1\Delta)$, $O_2(^3\Sigma)$, $O_2(^1\Sigma)$, Cl_2

k								Rates, cc/molecule–s
1	$O_2(^1\Delta)$	+	$O_2(^1\Delta)$	→	$O_2(^1\Sigma)$	+	$O_2(^3\Sigma)$	2.50e-17
4a	$O_2(^1\Sigma)$	+	H_2O	→	$O_2(^3\Sigma)$	+	H_2O	6.70e-12
11	I_2	+	$O_2(^1\Sigma)$	→	2I	+	$O_2(^3\Sigma)$	4.00e-12
13	I_2	+	$O_2(^1\Delta)$	→	I_2*	+	$O_2(^3\Sigma)$	7.00e-15
14	I_2	+	I*	→	I	+	I_2*	3.50e-11
15	I_2*	+	$O_2(^1\Delta)$	→	2I	+	$O_2(^3\Sigma)$	3.00e-10
16	I_2*	+	$O_2(^3\Sigma)$	→	I_2	+	$O_2(^3\Sigma)$	5.00e-11
17	I_2*	+	H_2O	→	I_2	+	H_2O	3.00e-10
18	I_2*	+	He	→	I_2	+	He	4.00e-12
19	I	+	$O_2(^1\Delta)$	→	I*	+	$O_2(^3\Sigma)$	7.80e-11
20	I*	+	$O_2(^3\Sigma)$	→	I	+	$O_2(^1\Delta)$	1.0277e-10*exp(−401.4/T)
23	I*	+	$O_2(^1\Delta)$	→	I	+	$O_2(^1\Sigma)$	1.00e-13
26	I*	+	H_2O	→	I	+	H_2O	2.10e-12

Table 3 Reduced oxygen–iodine reaction set; 8 reactions, 8 species: I, I*, I_2, I_2*, He, H_2O, $O_2(^1\Delta)$, $O_2(^3\Sigma)$

k								Rates, cc/molecule–s
13	I_2	+	$O_2(^1\Delta)$	→	I_2*	+	$O_2(^3\Sigma)$	7.00e-15
14	I_2	+	I*	→	I	+	I_2*	3.50e-11
15	I_2*	+	$O_2(^1\Delta)$	→	2I	+	$O_2(^3\Sigma)$	3.00e-10
17	I_2*	+	H_2O	→	I_2	+	H_2O	3.00e-10
18	I_2*	+	He	→	I_2	+	He	4.00e-12
19	I	+	$O_2(^1\Delta)$	→	I*	+	$O_2(^3\Sigma)$	7.80e-11
20	I*	+	$O_2(^3\Sigma)$	→	I	+	$O_2(^1\Delta)$	1.0277e-10*exp(−401.4/T)
26	I*	+	H_2O	→	I	+	H_2O	2.10e-12

One possible way of improving performance is to shift the location of the mirrors to more efficiently utilize the available gain curves. Calculations (not shown) indicate that substantial increases in power can be obtained for a variety of flow conditions by moving the leading edge of the mirror upstream and/or increasing the total mirror (or aperture) size.

Another possible way of improving performance at higher pressures may be to add different thickness spacer plates between the I_2 injectors and the nozzle throat. Calculations (not shown) indicate that the addition of the spacer plate enables the gain to build up in the subsonic portion of the nozzle, so that there is sufficient gain in the cavity region to lase. It appears that it should be possible to obtain a significant fraction of the baseline $\psi = 3$, $\beta = 0.016$ power of 4400 W with $\psi = 20$, $\beta = 0.050$ flow conditions with an appropriate choice of secondary He flow rate, spacer plate size, mirror location, and mirror size.

IV. Effects of Reduced Sets of Reactions and Species

To reduce the required computational time for two- and three-dimensional computational fluid dynamics (CFD) simulations, two reduced kinetic mechanisms were determined. The full 33-reaction, 12-species COIL kinetics package[13] is given in Table 1. Several reduced reaction/species sets were investigated. The two reduced mechanisms which showed the best agreement with the full mechanism were a 13-reaction, 10-species set, Table 2, and an 8-reaction, 8-species set, Table 3. The 8-reaction, 8-species set was obtained by eliminating all $O_2(^1\Sigma)$ reactions and removing Cl_2 from the flow. These three reaction sets were run for the nominal mixing case, $\psi = 3$, $\beta = 0.016$. Figure 10 shows that the gain curves of the two reduced mechanisms are in very good agreement with the full mechanism. The resulting power calculation from the 13-reaction, 10-species set was 1% higher than the full set. The resulting power calculation from the 8-reaction, 8-species set was 8% higher than the full set. For the purposes of reducing the computation time required by slow CFD codes, the 8-reaction, 8-species set is recommended because it quite adequately models the kinetics of the RADICL nozzle at nominal conditions. For relatively fast CFD codes (for example, those employing parabolized Navier–Stokes techniques), the 13-reaction, 10-species set is recommended because it retains the species $O_2(^1\Sigma)$ and Cl_2 and the reactions associated with $O_2(^1\Sigma)$.

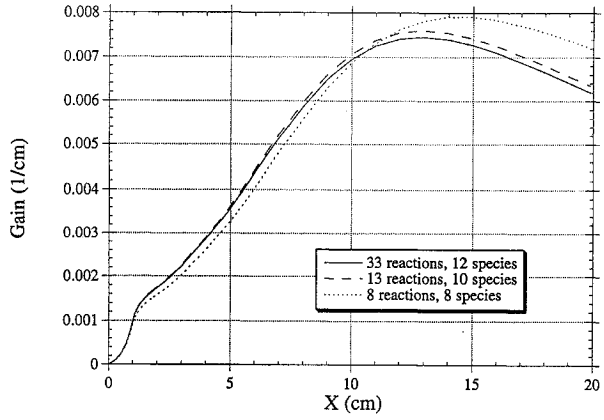

Fig. 10 Predicted gain vs distance for three different reaction/species sets; Blaze II parameters are a yield of 0.53 at $\psi = 3$ ($\beta = 0.016$ case), 0.08 H_2O, 12 × k_{18}, $J_{exp} = 1.1$, and $DCM_{exp} = 1.0$.

V. Concluding Remarks

The Blaze II chemical laser model was used to model chemical oxygen-iodine laser (COIL) performance at high pressure. First, this model was verified against the existing premixed RECOIL code which has been used in the past to model low-pressure COIL performance. The primary advantage to the Blaze II model is that it will perform mixing calculations; this is critical because mixing changes dramatically as the pressure in the device is increased and flow rates are altered.

The Blaze II chemical laser model was modified to perform mixing calculations for single slit nozzle geometries with side wall injection such as the oxygen–iodine RADICL nozzle. These modifications include the ability to compute mixing beginning in the subsonic portion of a subsonic/supersonic nozzle. Jet penetration is based on the momentum flux ratio of the secondary injectors to the primary oxygen flow. Blaze II was baselined to existing RADICL data. To obtain good agreement with power as a function of diluent ratio (ψ) data, the $I_2^* + He \rightarrow I_2 + He$ rate constant (k_{18} of Table 1) was increased by an order of magnitude (a factor of 12

best matched the data). Mixing COIL calculations for the RADICL nozzle indicated that higher iodine flow rates are necessary to obtain a significant fraction of the nominal performance as ψ is increased to raise the total pressure of the flow; this agrees with RADICL experimental data.

A significant performance increase for most RADICL flow conditions should be obtainable if the mirror leading edge is moved upstream from its present location and the mirror aperture is made larger. Calculations indicate that it should be possible to obtain a significant fraction of the baseline $\psi = 3$, $\beta = 0.016$ power of 4400 W with $\psi = 20$, $\beta = 0.050$ flow conditions with an appropriate choice of secondary He flow rate, spacer plate size, mirror location, and mirror size.

A genetic algorithm technique was implemented to determine a set of unknown parameters (yield, water vapor flow rate, rate constant k_{18}, jet expansion factor, and the DCM) which best matched Blaze II model predictions with experimental data. This is the first known application of the genetic algorithm technique for modeling lasers, chemically reacting flows, and chemical lasers. Now that these unknown parameters are established for the RADICL device, it may be possible to implement this genetic algorithm technique as a system design tool to optimize the RADICL performance as a function of any of the flow rates, mirror location, mirror size, spacer plate size, nozzle configuration, injector sizes, and other possible factors. This modeling procedure could possibly be used as a method to guide experiments to enhance the performance of the RADICL device at high pressure. For other chemical laser devices (COIL or HF), it may be possible to use the Blaze II model linked with a genetic algorithm driver as a system design tool to guide experiments for optimal performance as a function of flow rates, nozzle configuration, mirror position, etc.

Three-dimensional Navier–Stokes calculations are essential for understanding the details of the fluid mechanics, three-dimensional mixing and chemistry which occur in these extremely complex chemical laser devices. To reduce the number of equations that a three-dimensional Navier–Stokes model must solve, different reduced reaction/species sets were investigated. A 13-reaction, 10-species set was found that gave excellent agreement, and an 8-reaction, 8-species set gave very good agreement with the full reaction set. To minimize required computer time, the 8-reaction, 8-species set is recommended for use in slow CFD codes. For relatively fast CFD codes, the 13-reaction, 10-species set is recommended because it retains the species $O_2(^1\Sigma)$ and Cl_2 and the reactions associated with $O_2(^1\Sigma)$.

Acknowledgments

This work was supported by the Air Force under Contract F33615-89-C-2912. Many thanks to J. Shaw for providing the RADICL data, and to G. Hager, D. Plummer, L. Sentman, W. Solomon, and T. Madden for numerous useful conversations.

References

[1]Truesdell, K. A., Lamberson, S. E., and Hager, G. D., "Phillips Laboratory COIL Technology Overview," AIAA Paper 92-3003, July 1992.

[2]McDermott, W. E., "Singlet Delta Generator Performance—Overview," AIAA Paper 92-3005, July 1992.

[3]McDermott, W. E., "The Generation of Singlet Delta Oxygen—A Technology Overview," *Intense Laser Beams and Applications*, International Society for Optical Engineering, Vol. 1871, Los Angeles, CA, 1993, pp. 135–147.

[4]Thayer, W. J. I., "Sensitivity of the Uniform-Droplet Oxygen-Generator Output to Flow Conditions and Geometry," *Intense Laser Beams and Applications*, International Society for Optical Engineering, Vol. 1871, Los Angeles, CA, 1993, pp. 193–202.

[5]Copeland, D. A., Quan, V., Blauer, J. A., and Rodriquez, S. E., "Two-Phase Model of $O_2(^1\Delta)$ Production with Application to Rotating Disk Generators," *Intense Laser Beams and Applications*, International Society for Optical Engineering, Vol. 1871, Los Angeles, CA, 1993, pp. 203–228.

[6]Whitefield, P. D., Hagen, D. E., Trueblood, M. B., Barnett, W. M., and Helms, C., "Experimental Investigation of Homogeneous and Heterogeneous Nucleation Condensation Processes and Products in COIL," *Intense Laser Beams and Applications*, International Society for Optical Engineering, Vol. 1871, Los Angeles, CA, 1993, pp. 277–288.

[7]McDermott, W. E., "The Generation of Singlet Delta Oxygen: A Technology Overview," AIAA Paper 93-3220, July 1993.

[8]Copeland, D. A., McDermott, W. E., Quan, V., and Bauer, A. H., "Exact and Approximate Solutions of the Utilization and Yield Equations for $O_2(^1\Delta)$ Generators," AIAA Paper 93-3220, July 1993.

[9]Nowlin, M. L., and Heaven, M. C., "Spectroscopy and Energy Transfer Dynamics of I_2 Levels in the 1.0–1.3 eV range," *Intense Laser Beams and Applications*, International Society for Optical Engineering, Vol. 1871, Los Angeles, CA, 1993, pp. 290–303.

[10]Crowell, P. G., and Plummer, D. N., "Simplified Chemical Oxygen Iodine Laser (COIL) System Model," *Intense Laser Beams and Applications*, International Society for Optical Engineering, Vol. 1871, Los Angeles, CA, 1993, pp. 148–180.

[11]Sentman, L. H., Subbiah, M., and Zelazny, S. W., "Blaze II: A Chemical Laser Simulation Computer Program," Bell Aerospace Textron, T.R. H-CR-77-8, Buffalo, NY, Feb. 1977.

[12]Shaw, J., private communication, Phillips Laboratory, Kirtland AFB, Aug. 1993.

[13]Crowell, P. G., "RECOIL: A One-Dimensional Chemical Oxygen Iodine Laser Performance Model: Part I—Theory," RDA Letter No. 87-A/K-3-02-1079, Nov. 15, 1989.

[14]Carroll, D. L., Madden, T. J., Solomon, W. C., and Sentman, L. H., "High Pressure COIL: Final Report for 1993," Aeronautical and Astronautical Engineering Dept., Univ. of Illinois, TR 94-03, UILU Eng. 94-0503, Urbana, IL, May 1994.

[15]Shapiro, A. H., *The Dynamics and Thermodynamics of Compressible Fluid Flow*, Wiley, New York, 1953, pp. 99–100, 111, & 359.

[16]Committee, A. S. M. E. S. R., "Fluid Meters: Their Theory and Application: Part 1," 4th ed., American Society of Mechanical Engineers, New York, Aug. 1937, pp. 59–65.

[17]Cohen, L. S., Coulter, L. J., and Egan Jr., W. J., "Penetration and Mixing of Multiple Gas Jets Subjected to a Cross Flow," *AIAA Journal*, Vol. 9, No. 11, 1971, pp. 718–724.

[18]Crist, S., Sherman, P. M., and Glass, D. R., "Study of Highly Underexpanded Sonic Jet," *AIAA Journal*, Vol. 4, No. 1, 1966, pp. 68–71.

[19]Driscoll, R. J., private communication, Atlantic Research Corporation, Buffalo, NY, June 1991.

[20]Fristrom, R. M., and Westenberg, A. A., *Flame Structure*, McGraw-Hill, New York, 1965, Chap. 12.

[21]Schlichting, H., *Boundary-Layer Theory*, McGraw-Hill, New York, 1979, pp. 39–41.

[22]Driscoll, R. J., "Mixing Enhancement in Chemical Lasers, Part I: Experiments," *AIAA Journal*, Vol. 24, No. 7, 1986, pp. 1120–1126.

[23]Driscoll, R. J., "Mixing Enhancement in Chemical Lasers, Part II: Theory," *AIAA Journal*, Vol. 25, No. 7, 1987, pp. 965–971.

[24]Plummer, D. N., private communication, Logicon/RDA, Albuquerque, NM, Aug. 1993.

[25]Hager, G., private communication, Phillips Laboratory, Kirtland AFB, Aug. 1993.

[26]Sentman, L. H., Tsioulos, G., Bichanich, J., Carroll, D. L., Theodoropoulos, P., Gilmore, J., and Gumus, A., "A Comparative Study of cw HF Chemical Laser Fabry-Perot and Stable Resonator Performance," *Proceedings of the International Conference on Lasers '85*, edited by C. P. Wang, STS Press, McLean, VA, 1986, pp. 281–287.

[27]Sentman, L. H., Nayfeh, M. H., Renzoni, P., King, K., Townsend, S., and Tsioulos, G., "Saturation Effects in a cw HF Chemical Laser," *AIAA Journal*, Vol. 23, No. 9, 1985, pp. 1392–1401.

[28]Sentman, L. H., Carroll, D. L., Theodoropoulos, P., and Gumus, A., "Scale Effects in a cw HF Chemical Laser," Aeronautical and Astronautical Engineering Dept., Univ. of Illinois, TR 86-5, UILU Eng. 86-0505, Urbana, IL, Sept. 1986.

[29]Plummer, D. N., Heidner, R. F. I., and Perram, G., "The Proceedings from the 1987 Air Force Weapons Laboratory Conference on Chemical Oxygen-Iodine Laser (COIL) Kinetics (held on 11 August 1987)," RDA/Logicon, R&D Associates, Albuquerque, NM, March 1988.

[30]Holland, J. H., *Adaptation in Natural and Artificial Systems*, Massachusetts Inst. of Technology Press, Cambridge, MA, 1992.

[31]Goldberg, D. E., *Genetic Algorithms in Search, Optimization and Machine Learning*, Addison-Wesley, Reading, MA, 1989, pp. 2–6.

[32]Heaven, M. C., and Nowlin, M. L., "The Role of Excited Molecular Iodine in the Chemical Oxygen Iodine Laser," AIAA Paper 94-2430, June 1994.

[33]Heaven, M. C., private communication, Emory University, July 1994.